Universidad de Valladolid

ESCUELA DE INGENIERÍAS INDUSTRIALES

UNIVERSIDAD DE VALLADOLID

ESCUELA DE INGENIERIAS INDUSTRIALES

Grado en Ingeniería Química

Estudio de un separador líquido-vapor para concentrar una corriente con nanopartículas a escala de laboratorio

Autor:

Lanza Ruiz, Manuel

Responsable de Intercambio en la Uva:

Juan García Serna

University of Nottingham

Valladolid, Junio 2015.

TFG REALIZADO EN PROGRAMA DE INTERCAMBIO

TÍTULO: **Study of a knock-out drum to concentrate a stream with nanoparticles at bench scale**

ALUMNO: **Manuel Lanza Ruiz**

FECHA: 19/03/2015

CENTRO: **Department of Chemical & Environmental Engineering of the University of Nottingham**

TUTOR: **Edward Lester**

Table of contents

List of figures

List of tables

1. Abstract

In this project, a flash drum is going to be studied as a method to concentrate a stream with nanoparticles continuously at bench scale. Several aspects are going to be analysed, such as the removal of water produced in the flash, the dragging of product that is carried by the vapour and the hydrodynamic size of the nanoparticles.

The nanoparticles were synthesized by a hydrothermal method at high pressure in a counter-current nozzle reactor, patented by the University of Nottingham [1]. Afterward, the pressure was released and the stream was concentrated using a flash drum and separating the vapour from the liquid.

Several designs of the flash drum have been tested, for example providing the rig with more insulation or adding a band heater, obtaining better results in the separation of the liquid and vapour.

In some cases, the amount of solids carried by the vapour was measured as well in order to know the amount of product that is not possible to recover.

Keywords: metal oxide nanoparticles, hydrothermal synthesis, continuous countercurrent reactor, knock-out drum, supercritical water.

Resumen

En este Proyecto, se va a estudiar un separador líquido-vapor como un método para concentrar una corriente con nanopartículas de forma continua a escala de laboratorio. Se analizarán varios factores, como la eliminación de agua en el flash, el arrastre de producto que es arrastrado por el vapor y el tamaño hidrodinámico de las partículas.

Las nanopartículas fueron sintetizadas por un proceso hidrotermal a alta presión en un reactor contracorriente continuo, patentado por la Universidad de Nottingham [1]. Después, se liberó la presión y la corriente fue concentrada usando el tanque de flash y separando el vapor del líquido.

Se han probado varios diseños del separador, por ejemplo, aportando más aislamiento térmico al equipo o añadiendo un calefactor, obteniendo mejores resultados en la separación del líquido y vapor.

En algunos casos, la cantidad de sólidos arrastrados por el vapor fue medida también para saber la cantidad de producto que no es posible recuperar.

Palabras clave: nanopartículas de óxidos metálicos, síntesis hidrotermal, reactor contracorriente continuo, separador líquido-vapor, agua supercrítica.

2. Introduction

Throughout the last years, nanotechnology research has greatly progressed. Their possible applications are uncountable in the field of medicine, electronic, biology, chemistry, etc.

Several batch methods at bench scale have been developed in order to synthesise nanoparticles. However a batch method is not normally suitable for a production at industrial scale.

The hydrothermal synthesis has been demonstrated to present several advantages over other conventional methods in the manufacturing of advanced materials, such as nanoparticles. Some of these advantages can be used to give crystal symmetry, high product purity and homogeneity, narrow particle size distributions, single-step processes, dense sintered powders, fast reaction times, which means lowest residence time, as well as for the growth of crystals with polymorphic modifications [2].

When the particles have a nanometre size, in other words, a smaller size than 100 nm, the materials have different and interesting mechanical and physical properties. For example: increased mechanical strength, enhanced diffusivity or higher specific heat and electrical resistivity.

Figure 1 shows the application of the nanoparticles in different branches of science and technology.

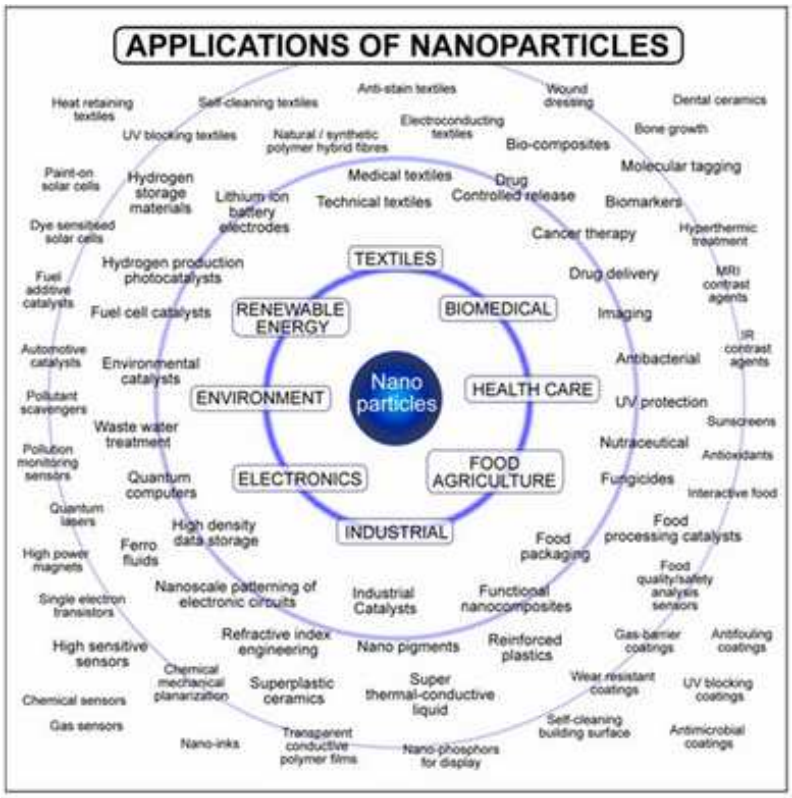

Figure 1. Applications of nanoparticles

Currently, the University of Nottingham is working on the European project SHYMAN (Sustainable Hydrothermal Manufacturing of Nanomaterials) [3]. They have been manufacturing a wide range of nanomaterials using a continuous counter current reactor by hydrothermal synthesis [1] [4-7].

One of the main objectives is to achieve a continuous process for the synthesis of nanoparticles at industrial scale. Several nanoparticles have already been synthesized at bench scale.

The hydrothermal synthesis presents several advantages over other conventional methods in the manufacturing of advanced materials, such as nanoparticles [2].

It has been demonstrated that it is possible to synthesise nanoparticles using a hydrothermal method. However the outlet stream from the reactor has a low concentration of nanoparticles, due to the low concentration of the feed metal salt solution that is possible to use currently.

The next step in the project is the investigation of new ways to concentrate these nanoparticles, which means, the elimination of water. One of these options is the use of a flash drum. This could be a cheap and easy method to eliminate a large part of the water from the outlet stream, while the stream would be cooled down at the same time without the need of using refrigeration.

In addition, the use of a knock out drum could be a method to have a controlled size particle of the aggregates of the nanoparticles, due to the quick cooling of the stream.

2.1. Supercritical water and reactions

Supercritical water hydrothermal synthesis involves the use of supercritical water to produce nano-sized metal oxide particles.

Supercritical water is in a state above the critical temperature (374 ºC) and pressure (22.1 MPa) of water. Above the critical point, the density of water varies greatly with little changes of temperature and pressure. Because of this, the other properties of the water change drastically as well, such as dielectric constant, which is a factor of the reaction rate, equilibrium, pH and solubility.

When water is heated towards its critical point, the dielectric constant drastically decreases and this changes its ionic solvent character to a solvent for non-ionic species. This behaviour can be seen in Figure 2.

K_w also increases, increasing the concentrations of H+ and OH-. These enhanced levels of OH- [8], allow a hydrolysis step of the metal salts that is followed by a dehydration step.

$$ML_x + xOH^- \rightarrow \mathrm{M(OH)\_} + xL^-$$

$$M(OH)_x \rightarrow \mathrm{MO}_{x/2} + \frac{x}{2}H_2O$$

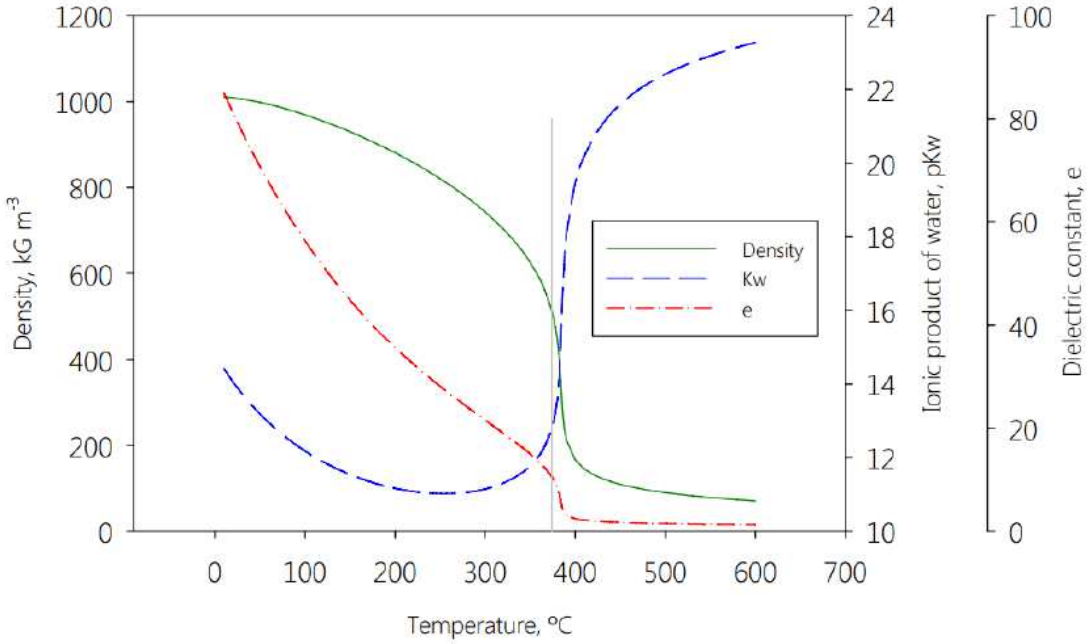

Figure 2. Properties of the water sub and supercritical

The kinetics increase greatly as well. In Figure 3 it is shown the Arrhenius plot of the first-order reaction rate constant of hydrothermal synthesis.

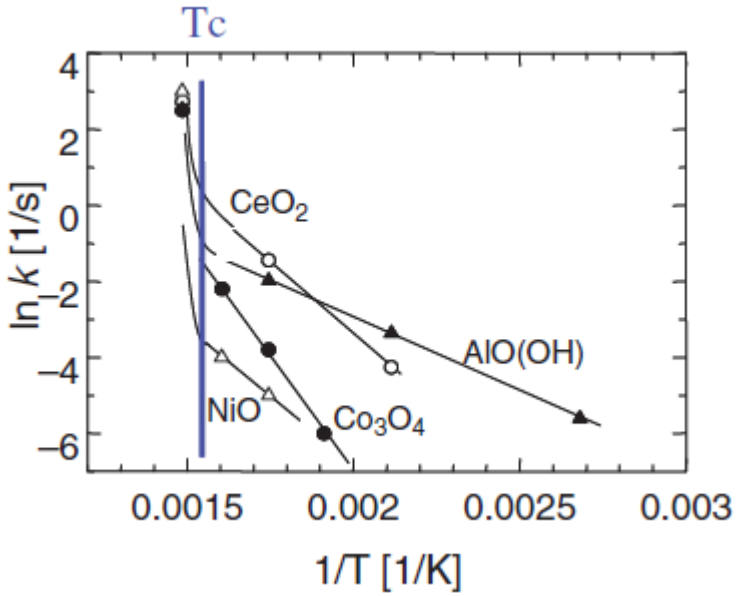

Figure 3. Kinetics of different metal oxides [9]

In order to heat the salt solution to the critical point of the water, salt solution is pumped towards the reactor and is mixed with high temperature water, which was fed to the top of the reactor. Then fast hydrothermal synthesis happens and the solubility of the salt is very low. In this way, high superstation of the metal oxide is obtained to form nanoparticles.

Due to limitations of the equipment, in this research project we will be working on the subcritical zone.

2.2. Nottingham nozzle reactor

The change of the hydrothermal synthesis from batch to continuous was first undertaken by the Professor Tadafumi Adschiri at Tohoku University in Sendai, Japan [8] [10]. They could synthesise several metal oxides using a continuous system.

The Clean Technology Research Group at the University of Nottingham carried out the development and optimisation of the hydrothermal continuous process. First, they used a T-piece for the reactor, but experiments run with this system were hindered by the unreliability of the process and a poor reproducibility. The problem was the accumulation and agglomeration within the reactor.

Then the SChEME ((School of Chemical, Environmental and Mining Engineering) investigated the fluid dynamic and mixing within the reactor using 2 techniques: LAI (Light Adsorption Imaging) modelling and CFD (Computer Fluid Dynamics). After using these techniques, the conclusion reached was that in spite of the low Reynolds number, the macromixing between the two inlets were turbulent due to the difference between their densities.

Then, they designed a new reactor design which exploited the natural convection forces that occur in the reactor. In the nozzle reactor the supercritical water is pumped towards the top of the reactor, whereas the cold metal salt aqueous stream is pumped towards the bottom of the reactor. The hot water stream heats the cold one, allowing the reactions and then the mixing flows upstream to the outlet of the reactor. [1]

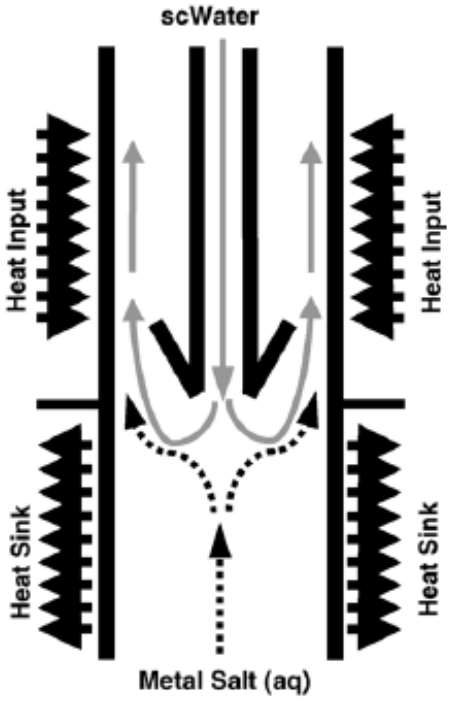

Figure 4. Schematic of the Nozzle Reactor design with ideal heating/cooling profile. [1]

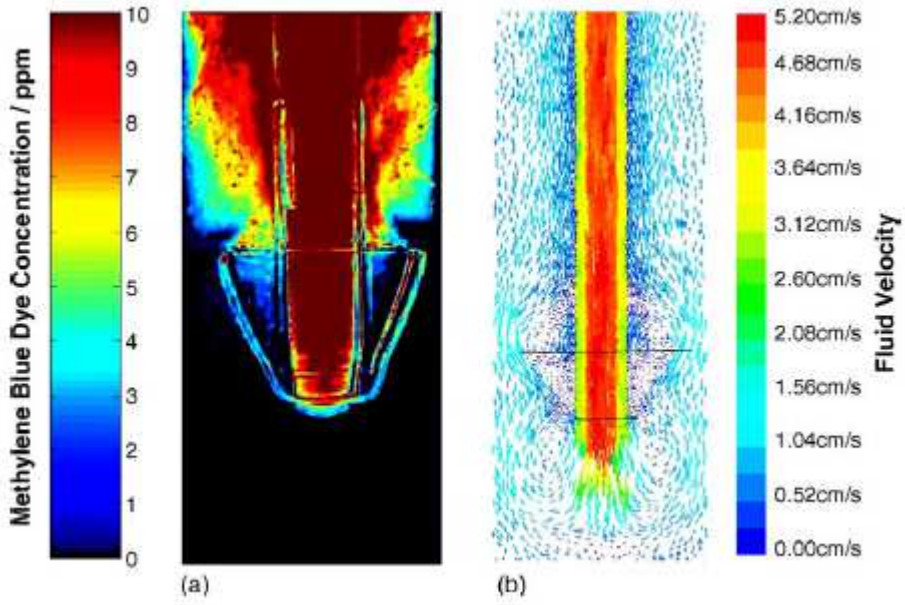

Figure 5. (a) LAI steady state concentration map of the Nozzle Reactor (b) steady state CFD simulation calculated using FLUENT. Both simulations at flow rates of 10 ml min^{-1} and 5ml min^{-1} for supercritical water and aqueous metal salt, respectively. [1]

The geometry of this *Nozzle Reactor* results in a better reliability and reproducibility than with the previous T-piece reactor, and problems, such us stagnant zones, flow partitioning and blockages were partially solved.

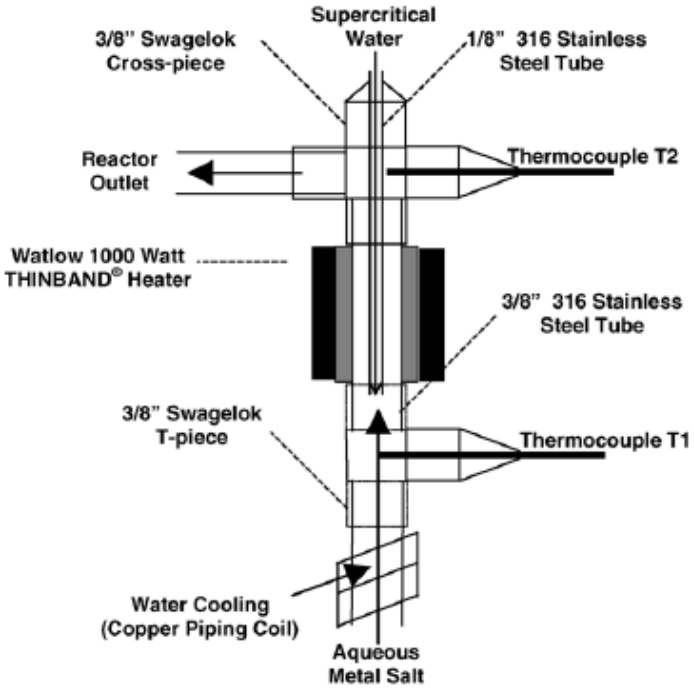

Figure 6. Construction of scWHS 'Nozzle Reactor' used in preliminary experiments [1]

The Nozzle Reactor was constructed using Swaglok® high pressure fittings; the outer tube consisted of a 3/8" tube (316 Stainless Steel, 0.065" wall thickness) and the inner tube consists of a 1/8" tube (316 Stainless Steel, 0.035" wall thickness).

This is the reactor that we will be using on this project to synthesize the nanoparticles.

3. Aims

The aim of this project is the study of a flash drum as a continuous method to concentrate a stream with nanoparticles at bench scale. If the results were favourable, this could be implemented at larger scale. For this study, several factors are going to be evaluated:

- The dragging of nanoparticles by the vapour. These nanoparticles are not dissolved in the water, they are in suspension. If this stream is flashed, a part of the product could be carried by the vapour due to the small size of the particles. This is an important aspect to take into account, as the solids that are carried are a product that is not possible to recover. At larger scale this could mean a big loss of product and consequently the unfeasibility of the flash drum as a separation method.

- The amount of water that it is possible to eliminate, which means, the amount of steam generated. Obviously the real separation in a flash drum will be lower than the theoretical one.

- The size of the aggregates that we can obtain. The nanoparticles tend to aggregate and create particles with a bigger hydrodynamic radius. If they aggregate too much, this can change their properties, in spite of the fact that they would still be considered “nano”. Apart from the particle size, it is interesting to control the size of the aggregates. The growth of the particles depends on the condition and on the particle. With a flash, the cooling is almost instantaneous and it may be possible to stop the growth of the aggregates. This may drive to a controlled size of particles.

4. Design of the flash drum

As we have discussed, it is necessary to concentrate the stream with nanoparticles after the reaction step, whose concentration is really low.

A simple and cheap way to achieve this is to use a knock-out or a flash drum, taking advantage of the enthalpy of the stream after the reactor. The idea is to depressurize the stream to near atmospheric pressure after the reactor, instead of cooling down the stream, and then separate the vapour generated during the flash.

In Figure 7, it is shown the P-H diagram of the water and a schematic of an isenthalpic expansion of a stream.

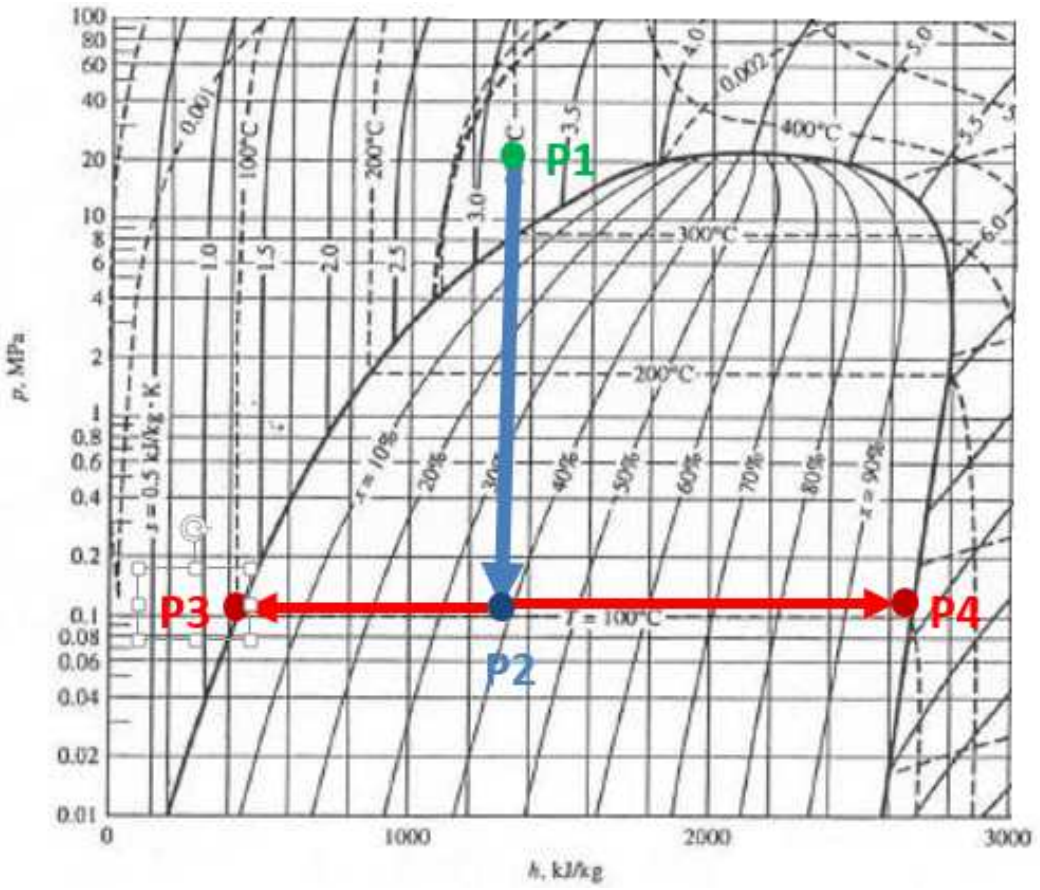

Figure 7. Schematic of the isenthalpic expansion that occurs in the flash step. A stream at 300ºC and 22MPa (P1) is depressurized with no change in the enthalpy to atmospheric pressure (P2). Then it is separated in a saturated liquid stream (P3) and a saturated vapour stream (P4).

4.1. Nanoparticles during a flash

The nanoparticles have a diameter smaller than 100 nm. With this size, it is easy to think that they would be carried by a stream of gas, even if the velocity was really low. However, we are considering a system with water and steam. A first assumption is that it would happen something similar to the formation of cloud droplets in the atmosphere.

According to Kelvin's equation, formation of cloud droplets requires formation of clusters of critical size to overcome evaporation. These clusters are known as CCN (cloud condensation nuclei) and they have the same order of magnitude as the nanoparticles [11].

In addition, at least the half of the mass flowrate is liquid flowrate, which enhances the formation of bigger droplets [12]. Therefore, it would be a good assumption that the nanoparticles will be inside the water droplets when the flash occurs.

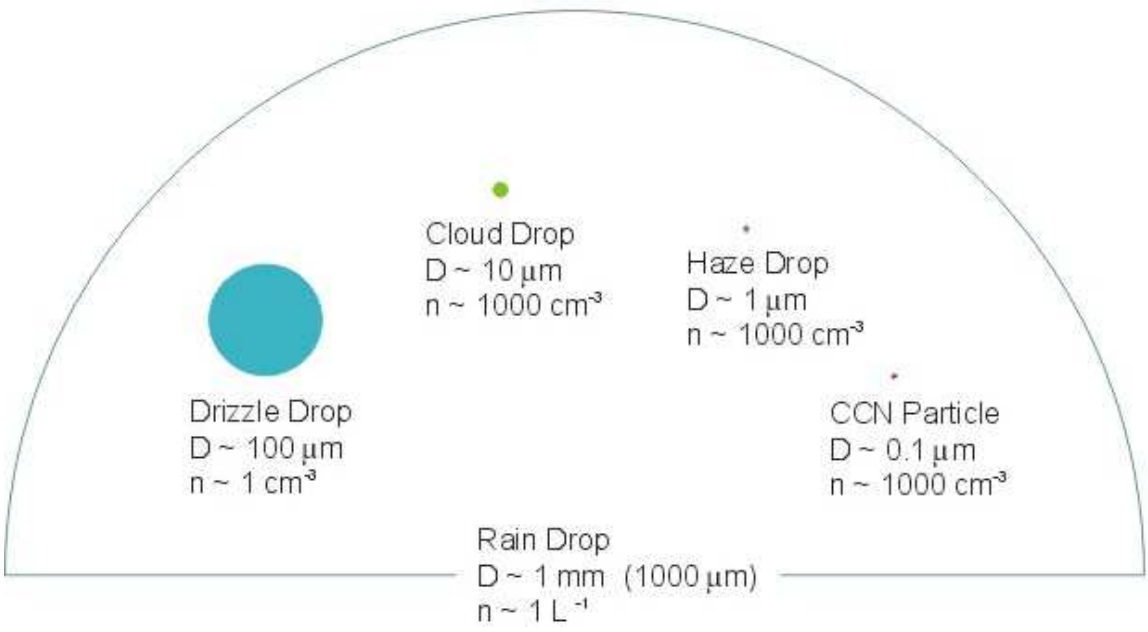

Figure 8. Relative sizes of cloud particles.

4.2. Terminal velocity of the gas

If we do not want the nanoparticles to be carried by the steam, we must study motion of the particles in a fluid. Considering we are working in a vertical flash drum, there are three forces to consider: the buoyant force, the drag force and the weight.

If a spherical particle is allowed to settle in a fluid under gravity, its velocity will increase until the accelerating force is exactly balanced by the resistance force (buoyant force and the drag force).

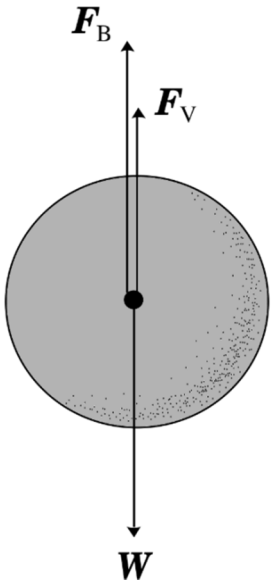

Figure 9. Schematic of the forces involved in the motion of a particle in a fluid, where F_B is the bouyanct force, F_V is the viscous force (drag force) and W is the weight of the particle.

If we want that the particles settle and go with the liquid stream instead of being carried by the vapour stream, then the weight force must be greater than the resistance force.

According to the bibliography, we have to know the drag coefficient in order to calculate the drag force [13]. The easiest way involves the use of two dimensionless groups. The first one is R'/ρu2, where:

$$\frac{R'}{\rho u^2} = \frac{F}{(\pi d^2/4)} \qquad (Equation\ 1)$$

In which R’ is the force per unit projected area of particle in a plane perpendicular to the direction of motion and d is the diameter of the particle. For a sphere, the projected area is a circle of the same diameter as the sphere.

R’/ρu2 is a form of drag coefficient, often denoted by the symbol C_D’. Frequently, a drag coefficient CD is defined as the ratio of R’ to 1/2ρu2.

$$C_D = 2C_D' = \frac{2R'}{\rho u^2}$$

The second dimensionless group is Reynolds number (Re’ or R_p), which is defined as:

$$Re_p = \frac{\rho u d}{\mu}$$

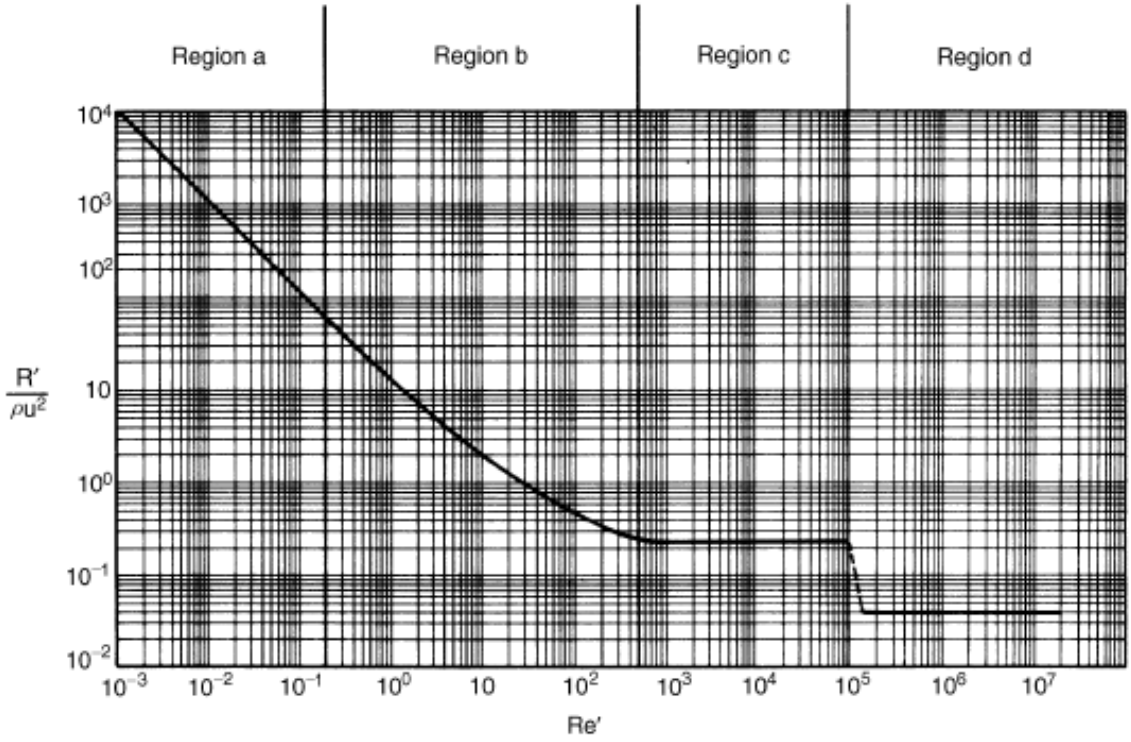

Figure 10. Re' vs ($R'/\rho u^2$)

Where *ρ* is the density of the fluid that the particle is in, *u* is the relative velocity of the fluid, *d* is the diameter of the particle and μ is the dynamic viscosity.

Depending on the Reynolds number we can distinguish between 4 zones where C_D' follows a different tendency. This is shown in Figure 10.

Further calculations on this study have demonstrated that we are working on the region b, if we are working at bench scale.

According to the bibliography, in the majority of the processes with a flash separation, the droplet size can vary from 10 µm to 5000 µm [14]. We can suppose a conservative value of 200 µm.

To calculate the terminal falling velocity of the particles, which means, the maximum velocity of the gas that lets the particles settle and fall down without being carried [13]:

$$F_{acceleration} = F_{friction}$$

$$F_{acceleration} = F_{weight} - F_{bouyant} = \frac{\pi \cdot D_p^3}{6} \cdot (\rho_s - \rho) \cdot g \qquad (Equation\ 2)$$

Where ρ_s is the density of the particles. We can assume that this density of these particles (droplets of water with nanoparticles inside) is approximately the density of liquid water, as the volume of the nanoparticles is much smaller than the volume of water in the droplets.

The drag force is a function of CD', which is a function of Re_p:

$$F_{drag} = f(C_D') \qquad (Equation\ 3)$$

$$C_D' = f(Re_p) \qquad (Equation\ 4)$$

According to the bibliography an approximate equation for the region b would be [15]:

$$C_D' = 12\ Re_p + \left(1 + 0.15 \cdot Re_p^{0.687}\right) \qquad (\ Equation\ 5)$$

Then:

$$\frac{\pi \cdot D_p^3}{6} \cdot (\rho_s - \rho) \cdot g = 3 \cdot \pi \cdot \mu \cdot D_p \cdot u_\infty \cdot \left(1 + 0.15 \frac{D_p \cdot \rho \cdot u_\infty}{\mu}\right) \quad (Equation\ 6)$$

Solving Equation 6:

$$\boldsymbol{u_\infty = 0.99\ m/s}$$

4.3. Diameter of the flash

Firstly, we have to know the total amount of vapour that we generate in order to calculate the velocity of the steam inside the flash drum.

We can assume that the outlet temperature of the reactor is 325ºC, the pressure is 240 bar and the depressurization is isenthalpic and adiabatic:

$$\Delta H\ (Water\ @\ 240bar\ and\ 325ºC) = \Delta H\ (Steam\ saturated\ @\ 1\ atm) + \Delta H\ (Liquid\ Water\ saturated\ @\ 1\ atm)$$

$$\boldsymbol{x = 0.465}$$

The thermodynamic data have been taken from [16].

We can remove, theoretically, almost half of the water from the stream.

In our bench rig we are pumping approximately 1.8 kg/h (30 ml/min), which means that in the flash we will be generating:

$$\dot{m} = 1.8\ \frac{kg\ water}{h} \cdot 0.465\ \frac{kg\ vapour\ generated}{kg\ water} = \boldsymbol{0.837\ \frac{kg\ vapour\ generated}{h}}$$

Then, the minimum diameter is the diameter where the velocity of the vapour is the same as the terminal falling velocity of the particles. Therefore, considering the amount of vapour that we will be generating:

$$\frac{\dot{V}}{\left(\pi\frac{D^2}{4}\right)} = u_\infty \qquad (Equation\ 7)$$

$$\dot{V} = 0.837\ \frac{kg\ vapour\ generated}{h} \cdot \frac{1\ m^3}{0.59034\ kg} = 1.4178\ \frac{m^3}{h}$$

Solving Equation 7:

$$\boldsymbol{D = 0.022\ m}$$

This is the minimum diameter to let the droplets of water fall down, assuming that the minimum diameter of the droplets is 200 micrometres.

4.4. Estimation of the droplet size

We assumed a diameter of the particles to design our bench scale flash drum. To know if our assumption is good enough, we will use the Harwell technique [17] [18].

This technique is one of the correlations for computing drop sizes and this allows us to get a rough estimation of the average drop size.

The Sauter mean diameter is defined as the diameter of a sphere that has the same volume/surface area ratio as a particle of interest. According to the Harwell equation, this diameter is calculated with the following formula:

$$(x)_{sa} = 1.91 \cdot Dt \cdot \frac{Re^{0.1}}{We^{0.6}} \cdot \left(\frac{\rho_g}{\rho_l}\right)^{0.6} \qquad (Equation\ 8)$$

Where $(x)_{sa}$ is the Sauter mean droplet diameter, and Re and We are the Reynolds and Weber number respectively. They are defined as:

$$Re = \frac{\rho_g v_t D_t}{\mu_g} \qquad We = \frac{\rho_g v_t^2 D_t}{\sigma}$$

Where D_t is the internal pipe diameter, ρ_g is the gas density, ρ_l is the liquid density, μ_g is the gas viscosity, v_t is the mean gas velocity in the pipe and σ is the interfacial surface tension.

The volume average diameter is related to the Sauter mean diameter through the following approximation:

$$(x)_{med} = 1.42 \cdot x_{sa} \qquad (Equation\ 9)$$

In our rig, the pipe before the flash drum is ½" outer diameter, which means 0.41" inner diameter (0.01041 m). Then, solving Equation 7:

$$v_t = 4.478\ m/s$$

$$Re = 2246.2 \qquad We = 2.08$$

Using Equation 8:

$$(x)_{sa} = 0.00032901\ m = 329\ \mu m$$

And solving Equation 9:

$$\boldsymbol{x_{med} = 467\ \mu m}$$

We have designed the flash for particles bigger than 200 µm. Theoretically, the average size of the droplets will be 467 µm. Therefore, with the designed flash drum we will be able to let most of the droplets settle and avoid the dragging of nanoparticles that are inside those droplets of water.

5. Description of the equipment

5.1. Reactor

The reactor used was the nozzle reactor of the University of Nottingham, previously described.

5.2. BPR

It is necessary to have a BPR that can withstand high temperature and high pressure. Normally, the stream after the reactor is cooled and it is possible to use a normal Tescom® BPR. However, the stream must keep that high enthalpy to produce a higher amount of vapour after the expansion in the BPR. In this way we can remove the water and concentrate the stream with nanoparticles.

The chosen valve is a EB1HP1 Equilibar® Precision Back Pressure, with upgraded FFKM O-Rings and a SS4 diaphragm. The maximum allowed temperature is 327 ºC and the maximum pressure is 5000 psig [19].

In addition, this BPR requires a high pressure cylinder that supplies an inert gas at high pressure to work. A BOC nitrogen 230 bar cylinder was used for this purpose.

Figure 11. Back Pressure Regulator from Equilibar®. Model EB1HP1.

The line from the BPR to the flash drum consisted of a 3/8” (316 Stainless Steel, 0.065” wall thickness) and 13 cm in length. This is a Swaglok® high pressure tube, although it would not be necessary, since after the BPR the pressure is approximately the same as the atmospheric pressure.

5.3. Flash drum

The flash drum was constructed using a Swaglok® high pressure fitting union tee. The three union of the tee piece had a 1” outer diameter (316 Stainless Steel 0.09” wall thickness). Therefore the inner diameter was 0.88”. As we calculated previously, this diameter should be enough to avoid the dragging of the droplets bigger than 200 µm.

The height of the tee piece is 3.96”.

Figure 12. T-piece that acts as the flash drum. Obtained from Swaglok® [20]

The line from the top of the flash drum to the vapour cooler consisted of a Swaglok® PFA (Perfluoroalkoxy alkane) ½” tube 90 cm in length. The line from the bottom of the flash drum to the liquid cooler consisted of a Swaglok® PFA ¼” tube. The maximum allowed temperature is 176 ºC and the maximum allowed pressure is 20.6 bar.

This is enough for our experiment, as we have to work at the boiling point of the water at atmosphere pressure, which means that the temperature is approximately 100 ºC.

Figure 13. PFA tubes from Swaglok®

5.4. Process flow diagram of the rig

In Figure 14 it is shown a PFD of the rig:

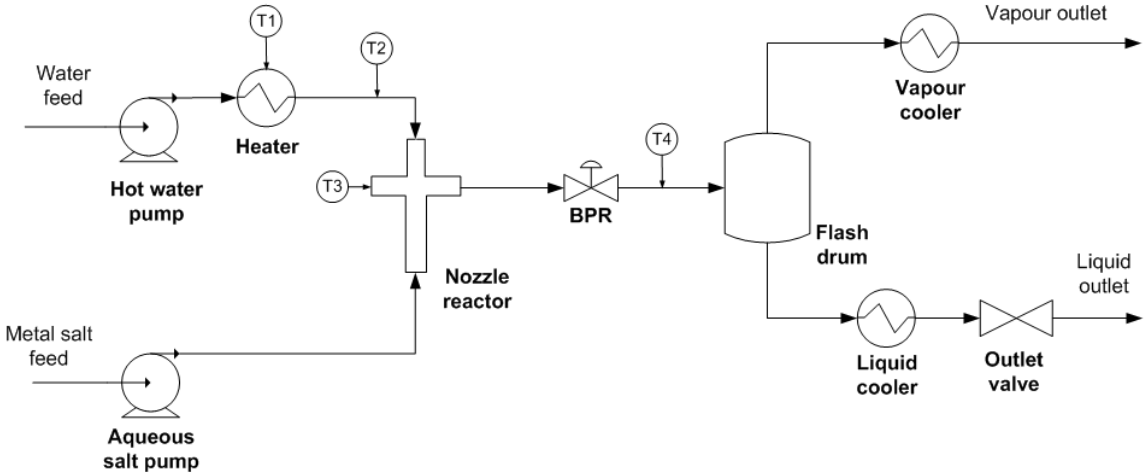

Figure 14. PFD of the rig used.

The outlet valve was a needle valve that was adjusted manually to assure a minimum level of liquid in the flash drum and to prevent some bubbles of the vapour from going with the liquid stream.

Where T1, T2, T3 and T4 represent the thermocouples used to indicate the temperature value at different points of the rig.

The thermocouple T1 indicates the temperature in the heater.

The thermocouple T2 is the thermocouple that indicates the temperature just before the reactor. We will assume that this temperature is the same as the temperature of reaction inside the reactor.

The thermocouple T3 indicates the temperature after the mixing point within the reactor, after the hot water stream and the aqueous cold stream are already mixed. We will assume that this temperature is the same as the temperature in the BPR.

The thermocouple T4 indicates the temperature after the BPR. This temperature must be near always the boiling point of the water at atmospheric pressure, which means approximately 100 ºC.

5.5. Photo of the rig

Figure 15. Photo of the flash rig

6. Experimental method

To carry out the experiment, a counter current reactor from Nottingham University has been used. Two pumps HPLC have been required to pump the water with a constant flow and high pressure. A heater was employed to increase the temperature of the downflow until 400 ºC degrees.

A back pressure regulator has been used to reduce the pressure and a T-piece has been used as a flash drum. To cool down the streams of liquid water and steam, two double pipe heat exchangers has been used. A needle valve at the outlet of the liquid stream was used to assure a minimum level of liquid in the flash drum.

Samples at the liquid outlet and the vapour outlet were collected at different temperatures and simultaneously, both flowrates were measured as well.

The efficiency of the removal of water has been defined as:

$$Efficiency\ (\%) = \frac{Water\ removed}{Theoretical\ maximum\ removal} \cdot 100 \qquad (Equation\ 10)$$

The particle size of the samples was measured by DLS analysis (Dynamic Light Scattering) using a Zetasizer Nano-ZS by Malvern Instruments.

Then, some samples were weighed and dried in an oven at 70ºC until all the water was evaporated. Then, they were weighed once again and the weight of the solids was calculated by gravimetric analysis, in both liquid and vapour samples.

6.1. Flash drum with no insulation

Firstly, some experiments were carried out in a rig without insulation. This would be the cheapest way, although this would produce a large heat loss that would make the efficiency of the flash drum be low.

6.1.1. Synthesis of titania (TiO_2)

Titanium dioxide, also known as titania, is widely used as a pigment. It can be used as a photocatalyst or in the manufacture of the composite materials for self-cleaning building walls [21].

The precursor used in this experiment to synthesize titania was Titanium (IV) bis (ammonium lactate) dihydroxide solution (50 %w, Sigma-Aldrich, UK) [22].

An aqueous solution containing 0.05 M Titanium (IV) bis (ammonium lactate) dihydroxide was pumped as the upflow, and deionized water was pumped through a heater, and then towards the nozzle reactor as the downflow.

The flowrate of water was 18 ml/min and flowrate of the aqueous solution was 9 ml/min. During the experiment, the total flowrate was measured, being slightly different every time. This could be due to disturbances in the system. However, we assumed that the ratio was 2:1 during the whole experiment, as we measured in the beginning.

The pressure was maintained at 3150 psi and the reaction temperature was gradually increased during the experiment from 300 ºC to 350 ºC.

6.1.2. Synthesis of hematite (Fe_2O_3)

Hematite or iron (III) oxide has several interesting properties, for example ferromagnetism. The magnetic properties of iron oxides have been exploited in a broad range of applications including magnetic seals and inks, magnetic recording media, catalysts, and ferrofluids [23].

Besides, it has been used in several biomedical applications, such as improving the quality of magnetic resonance imaging, hyperthermic treatment for malignant cells, site-specific drug delivery and the manipulation of cell membranes [24].

The precursor used to synthesize hematite in this experiment was Fe(NO3)3·9H2O (≥98 % Purity, Sigma Aldrich, UK). [25]

An aqueous solution containing 0.05 M $Fe(NO_3)_3$ was pumped as the upflow, and deionized water was pumped through a heater, and then towards the nozzle reactor as the downflow.

The flowrate of water was 17 ml/min and flowrate of the aqueous solution was 8.5 ml/min. During the experiment, the total flowrate was measured being slightly different every time. This could be due to disturbances in the system. However, we assumed that the ratio was 2:1 during the whole experiment, as we measured in the beginning.

The pressure was maintained at 3140 psi and the reaction temperature was gradually increased during the experiment from 200 ºC to 350 ºC.

6.1.3. Synthesis of ceria (CeO_2)

Cerium dioxide, also known as Ceria, has been investigated for its use as an antioxidant catalyst, as well as its different biomedical applications, such as the treatment of cancer [26][27].

The precursor used was $(NH_4)_2Ce(No_3)_6$ (≥98 % Purity, Sigma Aldrich, UK) [28].

An aqueous solution containing 0.05 M $(NH_4)_2Ce(No_3)_6$ was pumped as the upflow, and deionized water was pumped through a heater, and then towards the nozzle reactor as the downflow.

The flowrate of water was 15 ml/min and flowrate of the aqueous solution was 7.5 ml/min. During the experiment, the total flowrate was measured, being slightly different every time. This could be due to disturbances in the system. However, we assumed that the ratio was 2:1 during the whole experiment, as we measured in the beginning.

The pressure was maintained at 3150 psi and the reaction temperature was gradually increased during the experiment from 300 ºC to 350 ºC.

6.2. Flash with insulation in the reactor

In this case, insulation was provided to the reactor. This reduced the heat loss and the efficiency increased.

6.2.1. Synthesis of cobalt oxide

Cobalt oxide (Co_3O_4) nanoparticles have special interest in a wide range of applications, such as catalytic processes, manufacture of magnetic materials, energy storage and the use as a pigment [29].

The precursor used $(CH_3COO)_2Co{\cdot}4H_2O$ (<98% Purity, Sigma-Aldrich, UK) [30].

An aqueous solution containing 0.02 $(CH_3CO_2)_2Co$ was pumped as the upflow, and a solution containing 2.5% vol. H_2O_2 was pumped through a heater, and then towards the nozzle reactor as the downflow.

The flowrate of water was 20 ml/min and flowrate of the aqueous solution was 10 ml/min. During the experiment, the total flowrate was measured, being slightly different every time. This could be due to disturbances in the system. However, we assumed that the ratio was 2:1 during the whole experiment, as we measured in the beginning.

The pressure was maintained at 2750 psi and the reaction temperature was constant at 350ºC for 30 minutes.

After 30 minutes, the pressure started to fluctuate out of control and even increased over 3600 psi, consequently we turned off the rig. This was probably due to problems of blockage inside the rig.

6.3. Flash with insulation in the reactor and a band heater at the top of the flash drum

In this case, apart from the insulation of the reactor, a band heater was installed at the top of the flash drum. This maintained the temperature of the vapour stream at 100 ºC and increased the efficiency.

6.3.1. Synthesis of zirconia (ZrO_2)

Zirconium dioxide, or zirconia, is used as an anti-corrosion material in pumping components, in optical fibre technologies, in the manufacture of bioceramics and implant devices, in thermal barrier coatings, in electrolytes, anti-oxidant material, and in the manufacture of fluorescence materials [31].

The precursor used zirconium acetate solution (Zr ~ 16 %, Sigma-Aldrich, UK) [32].

An aqueous solution containing 0.05 M zirconium acetate was pumped as the upflow, and a solution containing 2.5% vol. H_2O_2 was pumped through a heater, and then towards the nozzle reactor as the downflow.

The flowrate of water was 20 ml/min and flowrate of the aqueous solution was 10 ml/min. During the experiment, the total flowrate was measured, and it was slightly different every time. This could be due to disturbances in the system. However, we assumed that the ratio was 2:1 during the whole experiment, as we measured in the beginning.

The pressure was maintained at 2700 psi and the reaction temperature was constant at 360ºC for 60 minutes.

7. Results and discussion

7.1. Flash drum with no insulation

7.1.1. Synthesis of titania (TiO2)

Table 1 shows the measured temperatures at different points and the flowrates of the liquid and the vapour streams after the flash, during the synthesis of titania.

Set point of the heater (ºC)	Temperature of the heater (ºC)	Reaction temperature (ºC)	Post-mixing temperature (ºC)	After BPR temperature (ºC)	Liquid flowrate (ml/min)	Vapour flowrate (ml/min)
320	321	300	233	98	23.5	2.36
346	347	325	253	98	23.5	4.71
355	356	348	283	98	18.5	7.1

Table 1. Temperatures and flowrates during the synthesis of titania.

Figure 16 shows the colour of the samples. It is possible to see that the higher the reaction temperature is, the stronger the colour of the samples is. Consequently, the higher the temperature is, the higher is the conversion. With the vapour samples, the colour is very clear, therefore the concentration must be really low.

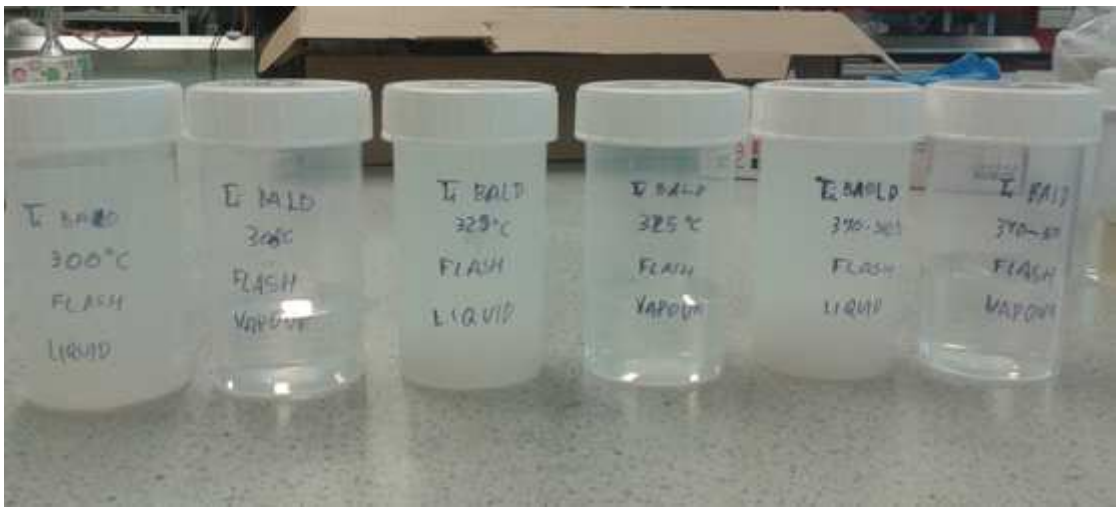

Figure 16. Samples of the liquid and the vapour collected during the synthesis of titania.

The hydrodynamic diameter was measured using DLS analysis. The results are shown in Table 2 and in Figure 17:

	Temperature (ºC)	Average diameter (nm)
Liquid	300	194.6
	325	282.6
	350	324.9
Vapour	300	116.3
	325	185.7
	350	98.63

Table 2. Hydrodynamic diameter of the samples collected during the synthesis of titania measured by DLS.

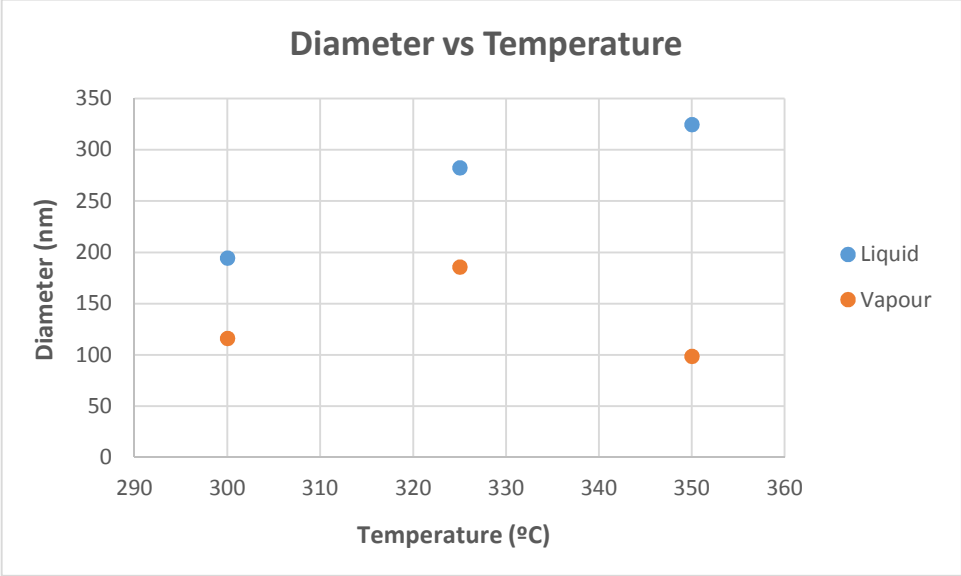

Figure 17. Diameter of the titania nanoparticles at different temperatures.

Normally, nanoparticles have a smaller diameter than 100 nm. As the results did not adjust to what it was expected, XRD (X-Ray Diffraction) was used to know about the crystallinity of the samples.

In Figure 18, it is shown the plot of the XRD analysis. It was impossible to make the analysis on the sample at 325ºC, since it formed aggregates too quickly and it was not possible to get powder for the XRD analysis.

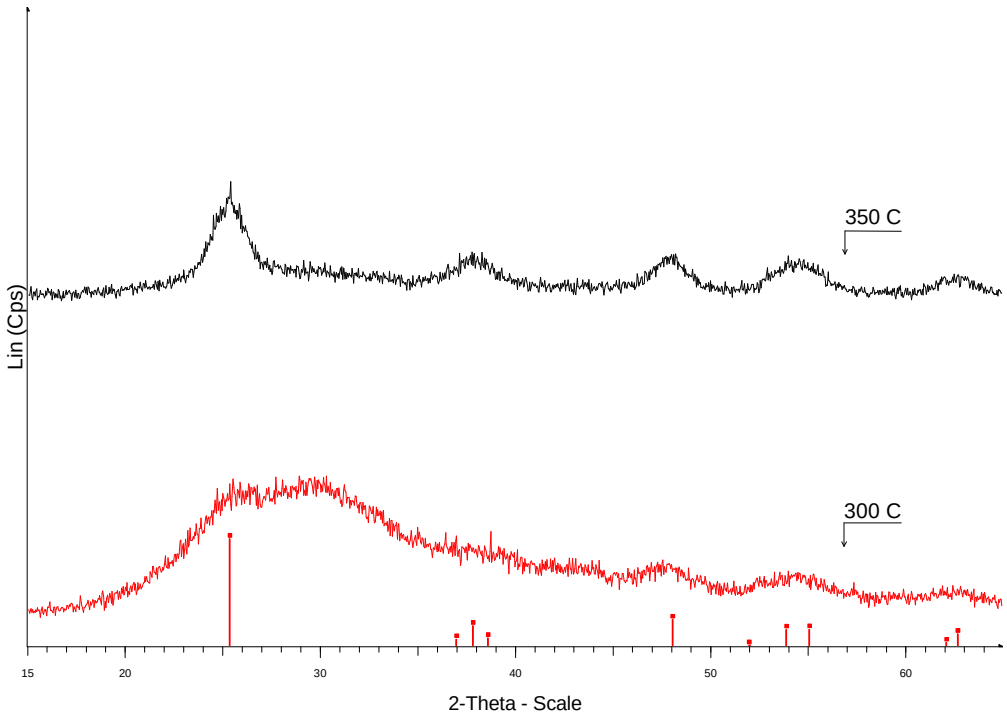

Figure 18. XRD of the titania liquid samples

It can be seen that there are peaks when 2θ is 25º, 38º, 48º, 54º and 55º. This indicates that there is titania in its anatase phase [33].

Maybe the large size of the particles could be due to a partial blockage in the rig that made the particles aggregate and increase their size.

7.1.2.Synthesis of hematite (Fe_2O_3)

Table 3 shows the measured temperatures at different points and the flowrates of the liquid and the vapour streams after the flash, during the synthesis of hematite.

Set point of the heater (ºC)	Temperature of the heater (ºC)	Reaction temperature (ºC)	Post-mixing temperature (ºC)	After BPR temperature (ºC)	Liquid flowrate (ml/min)	Vapour flowrate (ml/min)
215	228	200	150	70	23	-
274	271	250	190	93	23	-
320	323	300	240	98	21	2.88
344	346	325	266	98	18.5	4
354	360	352	293	98	19.5	5.6

Table 3. Temperatures and flowrates during the synthesis of hematite.

The flowrate of vapour was practically negligible when the reaction temperature was 200 ºC and 250 ºC.

Figure 19 shows the colour of the samples of the liquid. The samples have a darker red colour the higher the temperature of the reaction is, which means that the higher the temperature is, the higher the conversion is. With the vapour samples, shown in Figure 20, the colour is very clear, therefore the concentration must be really low.

Figure 19. Samples of the liquid collected during the synthesis of hematite.

Figure 20. Samples of the vapour collected during the synthesis of hematite

The hydrodynamic diameter was measured using DLS analyisis. The results are shown in Table 4 and in Figure 21:

	Temperature (ºC)	Average diameter (nm)
Liquid	200	20.9
	250	36.8
	300	43.2
	325	67.1
	350	88.5
Vapour	300	73.4
	325	73.0
	350	78.7

Table 4. Hydrodynamic diameter of the samples collected during the synthesis of hematite measured by DLS.

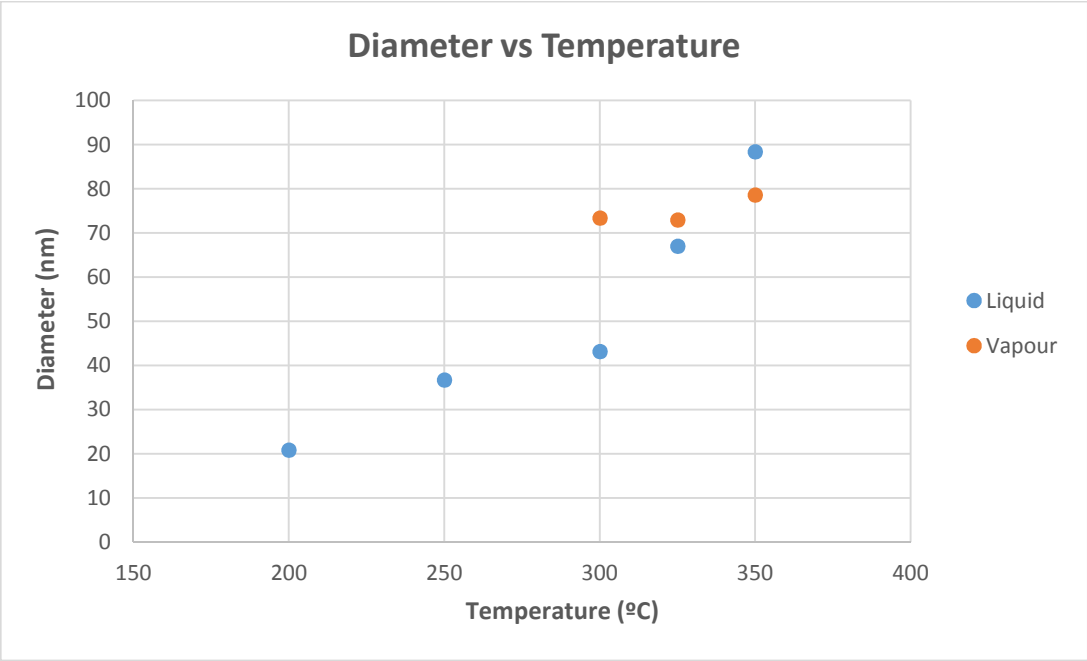

Figure 21. Diameter of the hematite nanoparticles at different temperatures.

It can be seen that the higher the temperature of reaction is, the larger the diameter of the particles is. Surprisingly, in the case of the vapour, the size is approximately constant.

Besides, the amount of solids in the vapour and in the liquid was measured. It was assumed that the conversion is high at those temperatures and the majority of the solids weighed by gravimetry were nanoparticles. This way we can do a rough estimation of the solids that are carried by the vapour, in other words, the percentage of product that we are losing in the vapour stream.

	Temperature of reaction (ºC)	Concentration (g/ml)	Flowrate (ml/min)	Solids (g/min)	% of the total of solids
Liquid	325	0.00133	23.5	0.03128	97.31
	350	0.00136	18.5	0.02519	95.74
Vapour	325	0.00018	4.71	0.00086	2.69
	350	0.00016	7.1	0.00112	4.25

Table 5.Mass balance of the solids of the both liquid and vapour samples of hematite

As it can be appreciated in Table 5, the higher the temperature is, the greater the dragging of the solids is, due to the fact that a larger quantity of vapour is generated and the velocity of the vapour is higher.

7.1.3.Synthesis of ceria (CeO_2)

Table 6 shows the measured temperatures at different points and the flowrates of the liquid and the vapour streams after the flash, during the synthesis of ceria:

Set point of the heater (ºC)	Temperature of the heater (ºC)	Reaction temperature (ºC)	Post-mixing temperature (ºC)	After BPR temperature (ºC)	Liquid flowrate (ml/min)	Vapour flowrate (ml/min)
320	319	300	240	98	21	3.5
345	346	325	270	98	18.8	5
354	355	350	292	98	18	5.5

Table 6. Temperatures and flowrates during the synthesis of ceria.

Figure 22 shows the colour of the liquid samples. The samples have a stronger colour the higher the temperature of the reaction is, which means that the higher the temperature is, the higher the conversion is.

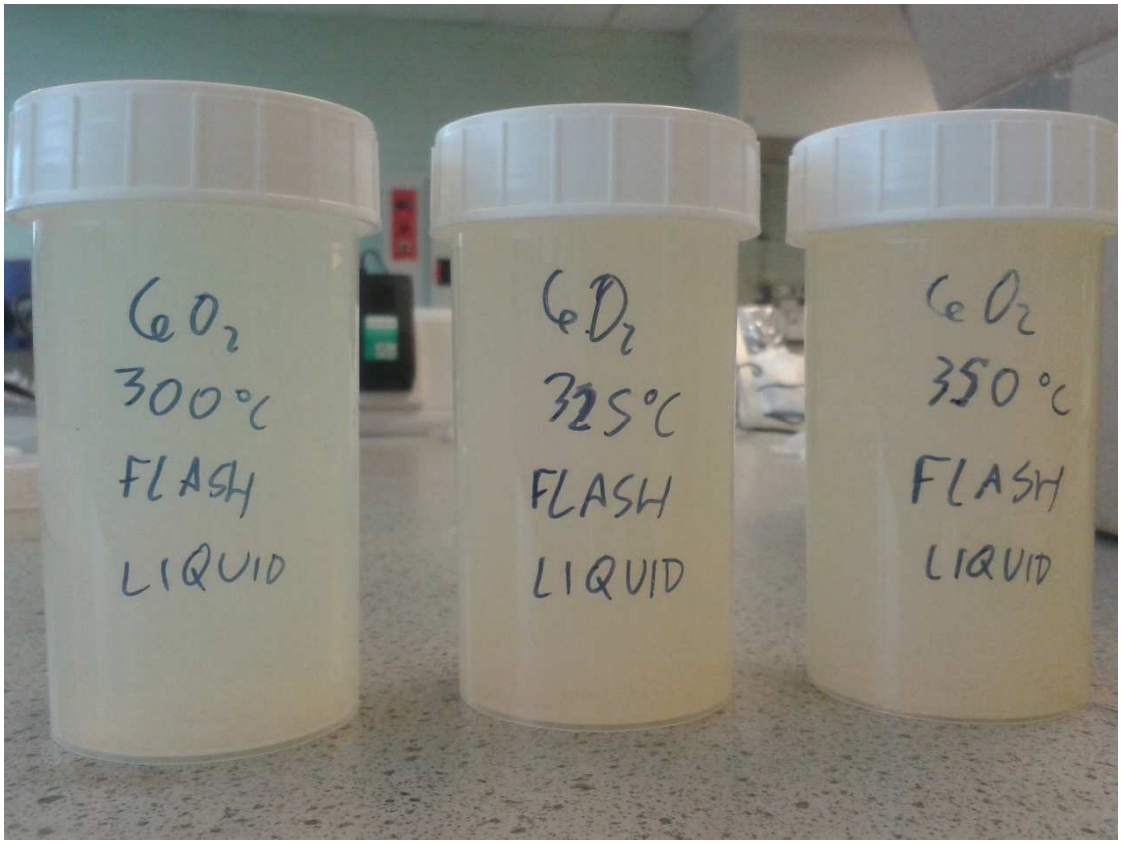

Figure 22. Samples of the liquid collected during the synthesis of ceria

The hydrodynamic particle size diameter was measured using DLS analysis. The results are shown in Table 7 and in Figure 23:

	Temperature (ºC)	**Average diameter (nm)**
Liquid	300	138.0
	325	116.8
	350	117.0
Vapour	300	111.2
	325	108.3
	350	101.2

Table 7.Hydrodynamic diameter of the samples collected during the synthesis of ceria measured by DLS.

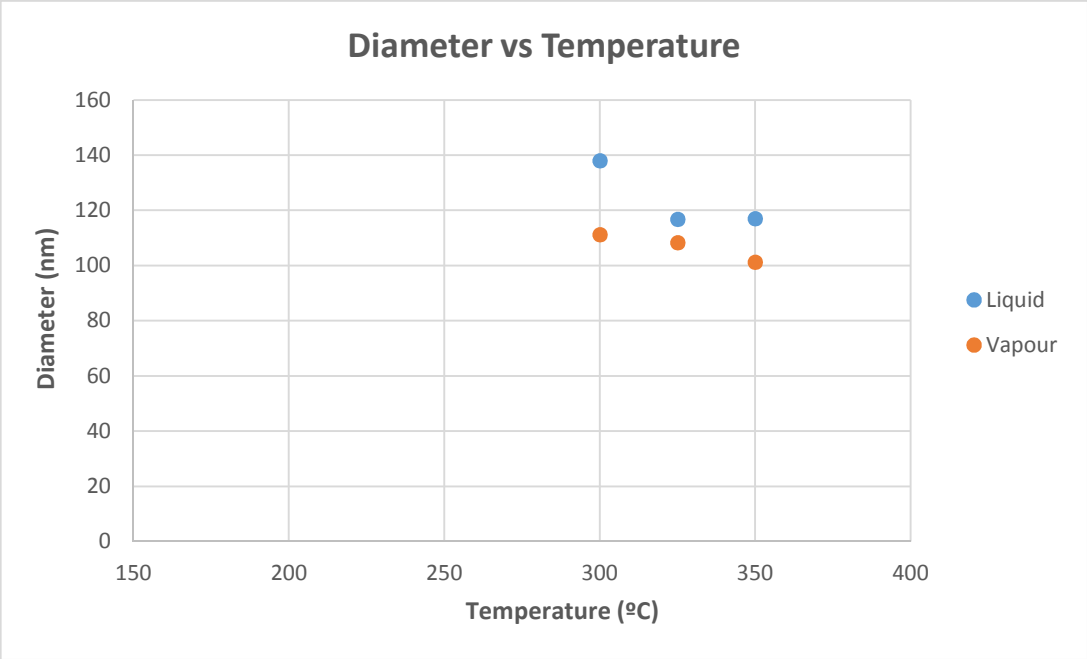

Figure 23. Diameter of the ceria nanoparticles at different temperatures.

Surprisingly, in this case it can be seen that the temperature barely influences the particle size.

As it was made with the hematite, it was measured the amount of the solids at the reaction temperature of 325 ºC.

	Temperature of reaction (ºC)	Concentration (g/ml)	Flowrate (ml/min)	Solids (g/min)	% of the total of solids
Liquid	325	0.00584	18.8	0.1099	97.26
Vapour	325	0.00062	5	0.0031	2.74

Table 8. Mass balance of the solids of the both liquid and vapour samples of ceria at 325ºC

7.1.4. Removal of water

Table 9 shows the percentage of removed water, and the efficiency of the flash without insulation at different temperatures. The calculations has been made with the data from Table 1, Table 3 and Table 6.

	Post mixing temperature (ºC)	Water removed (%)	Theoretical maximum removal (%)	Efficiency (%)
Titania (TiO_2)	233	9.13	26.18	34.86
	253	16.70	30.28	55.14
	283	27.73	36.70	75.57
Hematite (Fe_2O_3)	240	12.06	27.60	43.69
	266	17.78	33.01	53.85
	293	22.31	38.95	57.28
Ceria (CeO_2)	240	14.29	27.60	51.76
	270	21.01	33.87	62.03
	292	23.40	38.72	60.44

Table 9. % water removed and efficiency of the flash drum without insulation at different temperatures

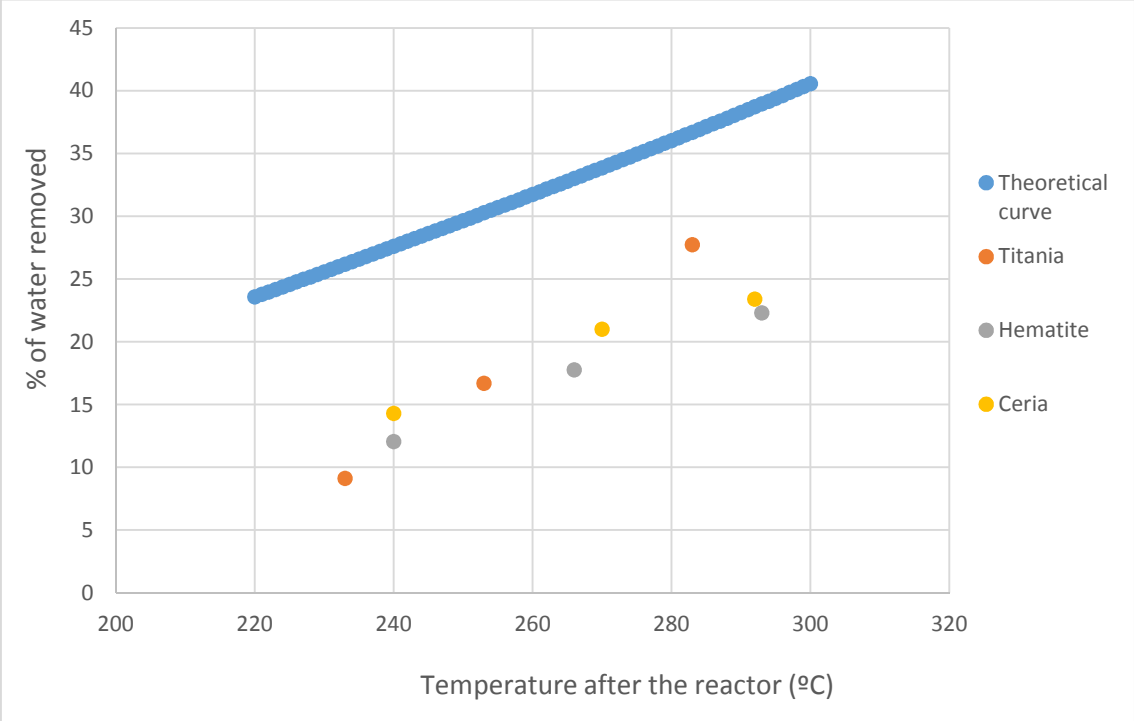

Figure 24. % of water removed at different temperatures using the flash without insulation

Figure 25 shows the efficiency of the flash drum without any insulation. The efficiency was defined previously by the Equation 10.

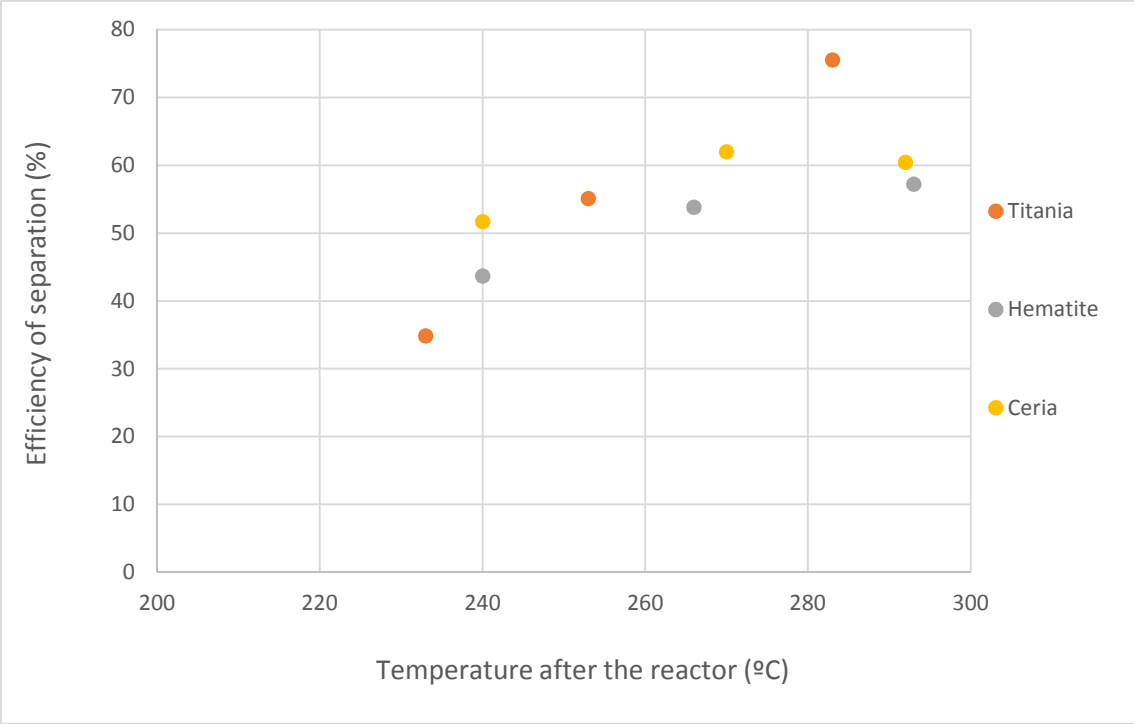

Figure 25. Efficiency of the removal of water at different temperatures using the flash without insulation

As it can be appreciated, the higher is the temperature, the higher is the efficiency. This is due to the fact that the higher the temperature is, the greater is the amount of vapour generated. Therefore the residence time along the pipes is lower and the heat loss is lower as well, which increases the efficiency.

7.2. Flash with insulation in the reactor

7.2.1. Synthesis of cobalt oxide

Table 10 shows the measured temperatures at different points and the flowrates of the liquid and the vapour streams after the flash, during the synthesis of cobalt oxide.

Set point of the heater (ºC)	Temperature of the heater (ºC)	Reaction temperature (ºC)	Post-mixing temperature (ºC)	After BPR temperature (ºC)	Liquid flowrate (ml/min)	Vapour flowrate (ml/min)
410	405	346	314	99	17.5	7.5
420	413	347	313	98	19	9

Table 10. Temperatures and flowrates during the synthesis of cobalt oxide.

Figure 26. Samples of the liquid and vapour collected during the synthesis of cobalt oxide

As it can be seen in Figure 26, the colour of the vapour sample is much clearer than the liquid sample, which means that the concentration of the vapour must be really low compared to the liquid.

The hydrodynamic particle size diameter was measured by DLS analysis. The results are shown in Table 11:

	Temperature (ºC)	**Average diameter (nm)**
Liquid	350	76.7
Vapour	350	167.1

Table 11. Hydrodynamic diameter of the samples collected during the synthesis of cobalt oxide measured by DLS.

As it can be seen, the particles size in the vapour is much higher than in the liquid. This could mean that during the dragging of the droplets, the particles keep aggregating inside the droplets.

In Table 12, it is shown the percentage of water removed (extracted from Table 10) and the calculated efficiency. It can be appreciated that the efficiency is higher than in the flash without insulation, since there is a smaller heat loss.

Post mixing temperature (ºC)	Water removed (%)	Theoretical maximum removal (%)	Efficiency (%)
314	30.00	43.92	68.30
313	33.96	43.68	77.75

Table 12. % of water removed and efficiency of the flash drum with insulation in the reactor during the synthesis of cobalt oxide

7.3. Flash with insulation in the reactor and a band heater at the top of the flash drum

7.3.1. Synthesis of zirconia (ZrO_2)

Table 13 shows the measured temperatures at different points and the flowrates of the liquid and the vapour streams after the flash, during the synthesis of zirconia.

Set point of the heater (ºC)	Temperature of the heater (ºC)	Reaction temperature (ºC)	Post-mixing temperature (ºC)	After BPR temperature (ºC)	Liquid flowrate (ml/min)	Vapour flowrate (ml/min)
411	362	362	336	100	15.5	13
414	362	362	337	100	16	13
411	362	362	335	100	15.5	13.5

Table 13. Temperatures and flowrates during the synthesis of zirconia.

In Figure 27, it is possible to appreciate that the liquid sample is cloudier than the vapour sample. The vapour is quite clear, therefore the concentration of nanoparticles must be really low.

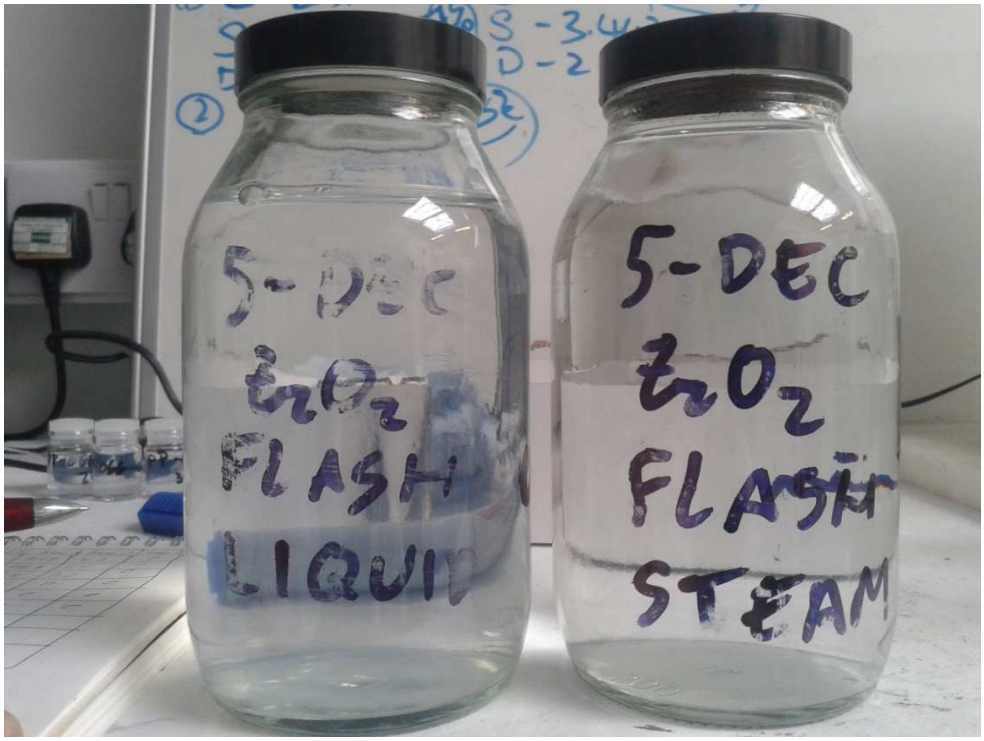

Figure 27. Samples of the liquid and vapour collected during the synthesis of zirconia

The hydrodynamic particle size diameter was measured using DLS analysis. The results are shown in Table 14:

	Temperature (ºC)	**Average diameter (nm)**
Liquid	360	19.2
Vapour	360	120.0

Table 14. Hydrodynamic diameter of the samples collected during the synthesis of cobalt oxide measured by DLS.

As happened with the cobalt oxide there is a great difference between the size of the particles in the liquid and in the vapour.

In Table 15, it is shown the percentage of water removed (extracted from Table 13) and the calculated efficiency:

Post mixing temperature (ºC)	Water removed (%)	Theoretical maximum removal (%)	Efficiency (%)
336	45.61	49.73	91.73
337	44.83	50.01	89.63
335	46.55	49.44	94.15

Table 15. % of water removed and efficiency of the flash drum with insulation in the reactor during the synthesis of zirconia

It can be appreciated that the efficiency is even higher than in the other designs, as apart from the insulation in the reactor, the band heater maintains the temperature in the flash drum.

8. Conclusions

It has been demonstrated that **it is possible to concentrate a stream with nanoparticles continuously by using a flash drum**. The amount of water removed was the **60-75%** of the theoretical maximum removal when we used a flash drum without insulation at the highest temperatures. When we provide insulation to the reactor, the efficiency of the flash drum increased up to **68-77%.** And when we provided a band heater to the flash drum as well, the efficiency of the flash drum increased again up to **89-95%.**

Regarding the dragging of solids, it has been evaluated during the synthesis of hematite and ceria. **At 350ºC, a 4.25% of the solids** was carried by the vapour. This is not a big percentage, but maybe, if water reached supercritical phase, the enthalpy of the stream would be higher, and a larger amount of vapour would be produced. Therefore, the velocity of the vapour would be higher and could carry a larger amount of nanoparticles. In those conditions, the amount of lost product could be too high and the flash would not be feasible.

In addition, we supposed a high conversion. Actually, a small part of the solids that we weighed is precursor that did not reacted. If we wanted some more accurate results, other analysis should be considered, such as ICP-MS (Inductively Coupled Plasma Mass Spectrometry). In this way, we could know the exact conversion.

The size of the particles was larger than it was expected. Specifically, it was **larger than 100 nm** in the titania and ceria samples. This could be due to a partial blockage in the rig. Surprisingly, the size of the particles in the vapour were larger than the particles in the liquid, which means that the agglomeration continues during the dragging of the particles. However, the size of the particles in the vapour is not interesting, as it is a product that we are losing and we are not going to recover.

9. Improvements of the rig

9.1. Dragging of the solids

To reduce the dragging of the solids, the diameter of the flash should be larger. However, this measure would result in a higher price of the flash drum. This is not a problem at bench scale, but at industrial scale, the cost of a flash drum is proportional to the diameter. This would require an economic evaluation.

Besides, it would be possible to install a demister at the top of the drum to enhance the coalescence of the droplets and let these fall down, in other words, to enhance the removal of liquid droplets carried by the vapour. This device reduces the diameter of the particles carried and therefore, increases the terminal falling velocity of the vapour.

9.2. Removal of water

First of all, we obtained better results when we provided insulation to the reactor. We obtained even better separation when we added a band heater at the top of the flash drum. However, using a heater means using an extra source of heat.

A better solution would be to provide insulation to all the lines from the reactor to the flash drum, and around the vapour line from the flash drum to the cooler of the vapour. This way the heat loss would be reduced and we may get efficiencies near 100%.

In addition, a thermocouple should be installed just before the BPR to reduce the error in the calculations of the efficiency, as we assumed that the post-mixing temperature was the same as the temperature in the BPR.

9.3. Particle size

We have obtained large particle sizes and some sizes over 100 nm. We must take into account that DLS measures the hydrodynamic diameter of the particles instead of the real diameter. We could get more accurate measurement using other technologies such as TEM (Transmission Electron Microscopy).

9.4. Other problems with the rig

Another problem was the difficulty of controlling a constant level in the flash drum, due to disturbances in the system. The liquid level was controlled manually adjusting the needle valve at the outlet of the liquid and it was not possible to know exactly the level of liquid since the flash drum is made of stainless steel.

The flash drum could be made of a transparent material. It would only have to resist atmospheric pressure and a temperature of 100ºC. Thus, it would be possible to notice what happens inside the flash drum and this allows to have a better control of the liquid level.

The maximum allowed temperature in the BPR is 327ºC, hence due to this limitation of the BPR, it was not possible to increase the temperature up to 373ºC in the reactor, to the point that we can get supercritical water. If we wanted to reach supercritical state, we would have to acquire some adequate equipment that can resist higher temperatures.

10. Bibliography

[1] Lester, E., Blood, P., Denyer, J., Giddings, D., Azzopardi, B. & Poliakoff, M. (2006). Reaction engineering: The supercritical water hydrothermal synthesis of nano-particles. *The Journal of Supercritical Fluids 37 209–214*

[2] http://www.shyman.eu/ Last time visited: 28/04/2015

[3] Byrappa, K., Adschiri, T. (2007). Hydrothermal technology for nanotechnology. *Progress in Crystal Growth and Characterization of Materials 53 117-166.*

[4] Gimeno-Fabra, M., Munn, A. S., Stevens, L. A., Drage, T. C., Grant, D.M., Kashtiban R. J., Sloan, J., Lester, E. & Walton, R. I. (2012). Instant MOFs: continuous synthesis of metal–organic frameworks by rapid solvent mixing. *Chem. Commun., 48, 10642–10644*

[5] Tang, S. Martín-Cortes, A., Khlobystov, A., Grant, D., Lester, E. The Impact of Blending Novel Forms of Hydroxyapatite from Continuous Hydrothermal Synthesis into Bone Scaffolds

[6] Poliakoff, M., Lester, E. (2013). The production and formulation of silver nanoparticles using continuous. *Chemical Engineering Science 85, 2–10*

[7] Dunne, P.W. Starkey, C.L., Gimeno-Fabra, M. & Lester, E. (2014). The rapid size- and shape-controlled continuous hydrothermal synthesis of metal sulphide nanomaterials. Nanoscale, 6, 2406

[8] Adschiri, T., Kanazawa, K., Arai, K. (1992). Rapid and continuous hydrothermal synthesis of metal oxide particles in supercritical water, *J. Am. Ceram. Soc. 75 1019.*

[9] Adschiri, T. (2007) Supercritical Hydrothermal Synthesis of Organic–Inorganic Hybrid Nanoparticles. *Chemistry Letters Vol.36, No.10*

[10] Adschiri, T., Hakuta Y. & Arai, K. (2000). Hydrothermal Synthesis of Metal Oxide Fine Particles at Supercritical Conditions. *Ind. Eng. Chem. Res.***,** *39, 4901-4901.*

[11] http://www2.physics.ox.ac.uk/sites/default/files/C5_PhysicsOfAtmospheresAndOceans_SectionA_Lecture3_WarmCloudMicrophysics_0.pdf Last time visited: 28/04/2015

[12] Azzopardi, B. J. (1997). Drops in annular two-phase flow. *Int. J. Multiphase Flow Vol. 23, Suppl., pp. 1-53.*

[13] Coulson & Richardson's Chemical Engineering. Volume 2, fifth edition. Particle Technology and separation processes. *Chapter 3*

[14] Couper, J.R., Penney, W. R., Fair, J.R., Walas, S.M. Chemical Process Equipment. Selection and design. Second edition. Chapter 18.

[15] SCHILLER, L. & NAUMANN, A.*Z.* (1933). Uber die grundlegenden Berechnungen der Schwerkraftaufbereitung. *Ver. deut. Ing.* 77 318.

[16] http://webbook.nist.gov/chemistry/fluid/ Last time visited: 28/04/2015

[17] Purnanto, M.H., Zarrouk, S.J. & Cater, J.E. (2013). *IPENZ TRANSACTIONS Volume 40, ISSN 1179-9293*

[18] Hoffmann, A.C. and Stein, L.E. (2007). Gas Cyclones and Swirls Tubes Principles, Design and Operation 2nd Edition. Springer, New York.

[19] http://www.equilibar.com/PDF/research-back-pressure-regulators.pdf Last time visited: 28/04/2015

[20] https://www.swagelok.com/ Last time visited 28/04/2015

[21] Kawasaki, S., Xiuyi, Y., Sue K., Hakuta, Y., Suzuki, A., Arai, K. (2009). Continuous supercritical hydrothermal synthesis of controlled size and highly crystalline anatase TiO2 nanoparticles. *Journal of Supercritical Fluids 50, 276–282*

[22] http://www.sigmaaldrich.com/catalog/product/aldrich/388165?lang=en&region=GB Last time visited 28/04/2015

[23] Teja, A.S. & Koh, P. (2009). Synthesis, properties, and applications of magnetic iron oxide nanoparticles. *Progress in Crystal Growth and Characterization of Materials 55, 22-45*

[24] Berry, C. C. & Curtis, A. S. G. (2003) Functionalization of magnetic nanoparticles for applications in biomedicine. *Journal of Physics D: Applied Physics, 36, R198–R206*

[25] http://www.sigmaaldrich.com/catalog/product/sial/216828?lang=en&region=GB Last time visited 28/04/2015

[26] Singh, S., Dosani, T., Karakoti, A.S., Kumar, A. Seal, S., Self, W.T. (2011). A phosphate-dependent shift in redox state of cerium oxide nanoparticles and its effects on catalytic properties. *Biomaterials 32, 6745-6753*

[27] Renu, G., Divya, R., Rani, V.V.D., Nair, S.V., Subramanian K.R.V. and Lakshmanan V.-K. (2012). Development of Cerium Oxide Nanoparticles and Its Cytotoxicity in Prostate Cancer Cells. *Advanced Science Letters Vol. 5, 1–9.*

[28] http://www.sigmaaldrich.com/catalog/product/sial/c3654?lang=en&region=GB Last time visited 28/04/2015

[29] Lester, E., Aksomaityte, G., Li, J., Gomez, S., Gonzalez-Gonzalez, J., Poliakoff, M. (2012). Controlled continuous hydrothermal synthesis of cobalt oxide (Co_3O_4) nanoparticles. *Progress in Crystal Growth and Characterization of Materials 58, 3–13.*

[30] http://www.sigmaaldrich.com/catalog/product/sial/403024?lang=en&region=GB Last time visited 28/04/2015

[31] Hobbs, H., Briddon, S., and Lester, E. (2009). The synthesis and fluorescent properties of nanoparticulate ZrO_2 doped with Eu using continuous hydrothermal synthesis. www.rsc.org/greenchem

[32] http://www.sigmaaldrich.com/catalog/product/aldrich/413801?lang=en&region=GB Last time visited 28/04/2015

[33] Mahdi, E.M., Hamdi, M., Meor Yusoff M. & Wilfred P. (2013). XRD and EDXRF Analysis of Anatase Nano-TiO_2 Synthesized from Mineral Precursors. *Advanced Materials Research Vol. 620 pp 179-185*